Mass-Analyzed Threshold Ionization Study of Vinyl Chloride Cation in the First Excited Electronic State Using Vacuum Ultraviolet Radiation in the 107−102.8 nm Range

Mina Lee and Myung Soo Kim*

National Creative Research Initiative Center for Control of Reaction Dynamics and School of Chemistry, Seoul National University, Seoul 151-742, Korea

Received: April 21, 2006; In Final Form: June 10, 2006

Vibrational spectrum of vinyl chloride cation in the first excited electronic state, $\tilde{A}^2A'$, was obtained by one-photon mass-analyzed threshold ionization (MATI) spectroscopy. Use of an improved vacuum ultraviolet radiation source based on four-wave sum frequency mixing in Hg resulted in excellent sensitivity for the MATI signals. From the MATI spectrum, the ionization energy to the $\tilde{A}^2A'$ state of the cation was determined to be 11.6667 ± 0.0006 eV. Nearly complete vibrational assignment for the MATI peaks was possible by utilizing the vibrational frequencies and Franck−Condon factors calculated at the DFT and TDDFT/B3LYP levels with the 6-311++G(3df,3pd) basis set. Geometry of the cation in the $\tilde{A}^2A'$ state was determined by Franck−Condon fitting of the MATI spectrum.

I. Introduction

Studying the properties of the excited electronic states of polyatomic molecules has been one of the research frontiers in chemistry.[1,2] Due to various experimental difficulties, however, there are not many polyatomic systems whose electronic states are well characterized. Compared to neutrals, it is even more difficult to study the excited states of polyatomic cations because most of the well established spectroscopic methods such as the infrared spectroscopy are not routinely applicable.[3,4] An exception is the photoelectron spectroscopy (PES), which can probe the excited hole states of a gas-phase polyatomic cation generated by removal of an electron from orbitals lying below the highest occupied molecular orbital (HOMO).[5,6] The fact that its resolution is not adequate for detailed spectroscopic study is its main disadvantage.

A molecule may be excited to a very high Rydberg state imbedded in the ionization continuum via resonance absorption and ionized by pulsed electric field. The technique which is called zero kinetic energy (ZEKE) photoelectron spectroscopy[7−9] or mass-analyzed threshold ionization (MATI) spectroscopy[10−12] depending on the particles detected, electrons or cations, has inherently better resolution than PES. This laboratory has been developing one-photon MATI technique utilizing vacuum ultraviolet (VUV) radiation generated by four-wave mixing in Kr or Hg.[13−15] In a conventional two-photon scheme, an intermediate excited state of the neutral should be present which is easily accessible with commercial pulsed dye lasers and is stable with respect to dissociation.[16−18] There are no such requirements in the present one-photon scheme. Also, it is to be mentioned that the two-photon scheme is virtually useless for the study of the excited states of cations because the scheme would usually involve a two-electron process. The Rydberg state generated by the two-photon scheme may be further excited by another photon to induce ionization. This technique, which is called the photoinduced Rydberg ionization spectroscopy, has been useful for the excited state study of molecular cations.[19,20] In contrast, studying excited hole states of molecular cations is rather straightforward with the one-photon scheme as long as VUV with appropriate wavelength is available. One-photon ZEKE/MATI spectroscopy has been practiced by several research groups,[8,21−23] most notably by Hepburn and Softley.[21−23] These groups reported spectroscopic results on relatively small molecules using VUV generated by four-wave sum or difference frequency mixings in Kr or Xe, which cover the wavelength ranges above 109 nm and below 92.3 nm.[21−23]

The ZEKE/MATI spectra provide accurate ionization energies as well as some vibrational frequencies of the corresponding ions. We recently reported that a good estimate of the geometry of a cation could be obtained via Franck−Condon fitting of a MATI spectrum.[24,25] This is all the more useful for polyatomic cations in excited electronic states because there is no guarantee that even the results from very extensive quantum chemical calculations are reliable in such cases.

Vinyl chloride is a major industrial product used mainly for PVC production.[26,27] It is considered to be a carrier for chlorine transported into the troposphere and stratosphere.[28,29] In this regard, photochemistry and dynamics of vinyl chloride have attracted much attention. Vinyl chloride cation in the first excited electronic state, $\tilde{A}^2A'$, is a particularly interesting system from a fundamental point of view also. Evidence was found in our previous charge exchange ionization[30] and photodissociation studies[31] that the state had a very long lifetime in the gas phase, probably much longer than several microseconds. A difficulty in the study of this state by one-photon MATI arises from the fact that VUV in the range 107−102.8 nm is needed. Even though sum frequency mixing in Hg can cover this range, it has been recognized that generating VUV with sufficient intensity in the 110−100 nm range is a difficult task.[32−34] The MATI spectrum of C_2H_3Cl in the energy range reported here was obtained by using a windowless Hg four-wave mixing light source developed in this laboratory.[15] Also reported will be the geometry of the cation estimated via Franck−Condon fitting of the spectrum.

* To whom correspondence should be addressed. Tel: +82-2-880-6652. Fax: +82-2-889-1568. E-mail: myungsoo@snu.ac.kr.

10.1021/jp062456u CCC: $33.50
Published on Web 07/12/2006

II. Experimental Section

C_2H_3Cl was purchased from Sigma Aldrich and used without further purification. The experimental setup was described in detail previously.[15] The gaseous sample at ambient temperature was seeded in He at the stagnation pressure of around 2 atm and supersonically expanded through a pulsed nozzle (diameter 500 μm, General Valve, Fairfield, NJ). The supersonic beam was then introduced to the ionization chamber through a skimmer (diameter 1 mm, Beam Dynamics, San Carlos, CA).

As has been mentioned already, VUV in the range 107−102.8 nm is needed to record the full vibrational spectrum of vinyl chloride cation in the $\tilde{A}^2A'$ state. Even though it is known that four-wave sum frequency mixing in Hg is capable of efficiently generating VUV radiation in the range 125−83 nm, going below 107 nm is still challenging because optical windows cannot be used in this range.[32−34] In our previous study on the first excited state of $C_2H_3Br^+$,[15] the windowless Hg light source with a series of capillaries developed in this laboratory was found to be very powerful in the 114−110 nm range. The same light source has been used in this work to record the MATI spectrum down to 102.8 nm.

Even though VUV in the desired spectral range could be generated by utilizing either the 6^1D_0-6^1S_0 or 7^1S_0-6^1S_0 transitions in Hg, the latter was used because the VUV output was stronger. ω_1 (312.8 nm) and ω_2 (337−300 nm) were generated by frequency doubling of dye laser outputs. Since ω_1 and ω_2 were close in wavelength, it was difficult to combine them using a dichroic mirror. Instead, a beam splitter which had 50% transmission for ω_1 and ω_2 was used at the cost of the power loss. Both were focused in the Hg cell for four-wave mixing ($\omega_3 = 2\omega_1 + \omega_2$). ω_3 was separated from the residual ω_1 and ω_2 by a home-built monochromator and overlapped collinearly with the molecular beam.

The experimental setup used for four-wave mixing also efficiently generates the frequency tripled output ($3\omega_1$). Since $3\omega_1$ was rather close to $2\omega_1 + \omega_2$ in the present case, the latter could not be clearly separated from the former by the home-built monochromator system. This resulted in the generation of an enormous amount of direct ions by $3\omega_1$. A weak spoil field was applied to remove these directly produced ions as much as possible. Then, an electric field of 250−300 V/cm was applied at 10−15 μs after the VUV to ionize the highly excited neutrals. The photoelectric current from a thin gold plate placed in the VUV beam path was used to calibrate the VUV intensity.

III. Computational Section

A. Quantum Chemical Calculation. Quantum chemical calculations were done for the vinyl chloride cation in the first excited electronic state at the TDDFT level using GAUSSIAN 98.[35] The size of the basis set was systematically increased until the basis set dependence became insignificant. Equilibrium geometry, Hessians, and vibrational frequencies were calculated for the cation in the first excited state. Similar calculations were done for the neutral in the ground electronic state at the DFT level using the same basis sets as above.

B. Franck−Condon Factor. The method of Sharp and Rosenstock which treats vibrations as harmonic was adopted to calculate the Franck−Condon factors.[36] In this calculation, the geometries, the vibrational frequencies, and the normal mode eigenvectors for the initial and final states are needed. Properties of the cation were assumed to approximate those of the ion core of a high Rydberg state. The following relation was used to account for the changes in normal coordinates upon ionization.

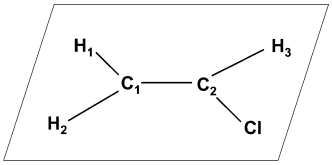

Figure 1. Atomic numbering of C_2H_3Cl.

$$\mathbf{Q}'' = \mathbf{J}\mathbf{Q}' + \mathbf{K} \tag{1}$$

Here, $\mathbf{Q}''$ and $\mathbf{Q}'$ are the normal coordinates for the neutral in the ground state and the cation in the first excited states, respectively, **J** is the Duschinsky matrix representing changes in the normal mode pattern, and **K** is a matrix representing changes in the equilibrium geometry upon ionization. Internal coordinates used in the calculation of these factors were five interatomic distances $r(C_1C_2)$, $r(C_1H_1)$, $r(C_1H_2)$, $r(C_2H_3)$, and $r(C_2Cl)$, four bond angles $\angle H_1C_1C_2$, $\angle H_2C_1C_2$, $\angle C_1C_2H_3$, and $\angle C_1C_2Cl$, and three dihedral angles $\angle H_1C_1C_2H_3$, $\angle H_2C_1C_2H_3$, and $\angle H_1C_1C_2Cl$. Atomic numbering is shown in Figure 1. From **J** and **K**, the following **C** and **D** matrices were evaluated.

$$\mathbf{C} = 2\Gamma'^{1/2}[\mathbf{J}^\dagger\Gamma''\mathbf{J} + \Gamma']^{-1}\Gamma'^{1/2} - \mathbf{1} \tag{2}$$

$$\mathbf{D} = -2\Gamma'^{1/2}[\mathbf{J}^\dagger\Gamma''\mathbf{J} + \Gamma']^{-1}\mathbf{J}^\dagger\Gamma''\mathbf{K} \tag{3}$$

Here, Γ' and Γ'' are diagonal matrices which have the vibrational frequencies of the cation and the neutral, respectively, as the diagonal elements. The explicit expressions for the intensities of vibrational peaks relative to that of the 0−0 band are as follows.

$$\mathrm{FCF}(i) = D_i^2/2 \quad i \text{ mode fundamental} \tag{4}$$

$$\mathrm{FCF}(i,j) = (2C_{ij} + D_iD_j)^2/4 \quad i,j \text{ modes combination} \tag{5}$$

The intensities of the fundamental peaks are determined by **D** which is more influenced by geometry change (**K** matrix) than by mode−mode coupling (**J** matrix), while both of these affect the intensities of the combination and overtone peaks.

IV. Results

A. Quantum Chemical. In all the quantum chemical calculations performed at the DFT or TDDFT/B3LYP levels using various basis sets, the vinyl chloride neutral in the ground electronic state and the cations in the ground and first excited electronic states have been found to have planar symmetry, C_s. Considering the valence orbitals only, the electron configuration of the ground-state neutral is $\cdots(1a'')^2(7a')^2(2a'')^2$. Here $2a''$ is a π orbital of C=C bonding with some C−Cl antibonding character, and $7a'$ and $1a''$ are chlorine 3*p* nonbonding orbitals parallel and perpendicular to the molecular plane, $n(\mathrm{Cl}\ 3p_{\|})$ and $n(\mathrm{Cl}\ 3p_{\perp})$, respectively.[37] The ground and first excited states of the cation are formed by the removal of an electron from $2a''$ and $7a'$, respectively, resulting in $\tilde{X}^2A''$ and $\tilde{A}^2A'$. The geometry of the cation in the $\tilde{A}^2A'$ state calculated at the TDDFT/B3LYP level using the 6-311++G(3df,3pd) basis set is shown in Table 1 together with the neutral geometry calculated at the DFT/B3LYP level using the same basis set. Since the $\tilde{A}^2A'$ state of the cation is formed by the removal of an electron from a nonbonding orbital, $n(\mathrm{Cl}\ 3p_{\|})$, the cation structure in this state is expected to be similar to that of the neutral as was the case for vinyl bromide investigated previously.[15] Calculated results

TABLE 1: Experimental and Calculated (DFT/B3LYP/6-311++G(3df,3pd)) Geometries of the Vinyl Chloride Neutral in the Ground State and Those of the Cation in the $\tilde{A}^2A'$ State Obtained by Calculation (TDDFT/B3LYP/6-311++G(3df,3pd)) and Franck−Condon Fitting

	neutral ($\tilde{X}^1A'$)		cation ($\tilde{A}^2A'$)			
C_s	exp.[a]	DFT/B3LYP	TDDFT/B3LYP		Franck−Condon fitting[b]	
			Bond Length (Å)			
C_1-C_2[c]	1.333	1.320	1.323	(0.002)[d]	1.339	± 0.001
C_2-C_l	1.726	1.737	1.755	(0.018)	1.762	± 0.002
C_1-H_1	1.079	1.081	1.083	(0.001)	1.083[e]	
C_1-H_2	1.086	1.080	1.080	(0.000)	1.080[e]	
C_2-H_3	1.080	1.080	1.093	(0.013)	1.091	± 0.001
			Bond Angle (deg)			
$C_1-C_2-C_l$	122.7	123.6	125.1	(1.6)	120.4	± 0.1
$C_1-C_2-H_3$	123.1	123.9	127.9	(4.0)	129.7	± 0.5
$C_2-C_1-H_1$	119.6	119.4	117.2	(−2.2)	117.4[f]	
$C_2-C_1-H_2$	121.1	122.5	124.4	(1.9)	123.0[f]	

[a] Microwave spectroscopic data in ref 45. [b] Determined via Franck−Condon fitting of the MATI spectrum using eigenvectors obtained at the TDDFT/B3LYP level with the 6-311++G(3df,3pd) basis set. [c] Atomic numbering shown in Figure 1. [d] Geometry change upon ionization. [e] Values taken from TDDFT/B3LYP results. [f] Values estimated by assuming that the differences between the calculated and experimental data are the same in the neutral and in the cation.

TABLE 2: Vibrational Frequencies (in cm^{-1}) and Their Assignments for Vinyl Chloride Cation in the First Excited Electronic State ($\tilde{A}^2A'$)

				theoretical			MATI	
mode	symm	neutral[a]	PES[b]	freq[c]	int[d,e]	in.[e,f]	freq	int[e]
1	a'	3120		3262	0.002	0.002	3122	0.003
2	a'	3037		3160	6.0×10^{-5}	6.7×10^{-5}		
3	a'	3086		3043	0.007	0.007	2883	0.007
4	a'	1608		1628	3.1×10^{-4}	0.003	1546	0.003
5	a'	1371		1421	4.0×10^{-4}	4.8×10^{-4}		
6	a'	1279	1160	1227	0.147	0.194	1172	0.194
7	a'	1030		951	7.3×10^{-6}	0.001		
8	a'	720	520	572(−6)	0.032	0.114	524(−6)	0.113
9	a'	398	300	303(−1)	0.116	0.018	259(−2)	0.018
10	a''	896		1021	0	0		
11	a''	941		867	0	0		
12	a''	620		598	0	0	558	0.009
9^2				606	0.001	0.011	494(−4)	0.017
12^2				1196	0.002	0.002	1125	0.014
$6^1 8^1$				1799	0.003	0.017	1687(−6)	0.009
6^2				2454	0.007	0.014	2322	0.014
$4^1 6^1$				2855	1.5×10^{-4}	0.001	2702	0.002

[a] Reference 40. [b] Reference 37. [c] Calculated at the TDDFT/B3LYP level with the 6-311++G(3df,3pd) basis set. Numbers in parentheses are isotopic shifts for $C_2H_3{}^{37}Cl^+$. [d] Intensities calculated with molecular parameters obtained at the TDDFT/B3LYP level with the 6-311++G(3df,3pd) basis set. [e] Normalized to the intensity of the 0−0 band. [f] Determined via Franck−Condon fitting. See text for details.

showed that the most significant change in bond length upon ionization occurred for the C−Cl bond and for the $\angle C_1C_2H_3$ bond angle, again in agreement with the vinyl bromide case.[15] Unlike the latter case, however, the C_2-H_3 bond length was observed to increase noticeably by as much as 0.013 Å. A close inspection of the calculated results showed that the $7a'$ nonbonding orbital had a slight σ bonding character with respect to C_2-H_3. Hence, based on the Franck−Condon principle, one expects that the MATI spectrum would be dominated by the 0−0 band and that the C−Cl stretching and CCH bending fundamentals would be more prominent than other vibrational features. However, unlike vinyl bromide, there is a chance to observe C−H stretching modes. The calculated vibrational frequencies of the cation in the $\tilde{A}^2A'$ state are listed in Table 2 together with the assignment of the MATI peaks which will be presented later.

B. Ionization Energy. One-photon MATI spectra of the vinyl chloride recorded by monitoring $C_2H_3{}^{35}Cl^+$ and $C_2H_3{}^{37}Cl^+$ generated in the $\tilde{A}^2A'$ state are shown in Figure 2. The most intense peak at around 94 091 cm^{-1} in the MATI spectrum of $C_2H_3{}^{35}Cl$ corresponds to the 0−0 band of the $\tilde{A}^2A'$ state. As is well-known for ZEKE/MATI spectroscopy, the ionization onset position is influenced slightly by the electric field present during the time spanning excitation and ionization.[38,39] To correct for this effect, the 0−0 peak position was measured under various field conditions, and the results were extrapolated to the zero field limit. The ionization energies to the $\tilde{A}^2A'$ state of $C_2H_3{}^{35}Cl^+$ and $C_2H_3{}^{37}Cl^+$ thus determined are listed in Table 3. These are in agreement with the high-resolution PES results[37] within error limits.

C. Vibrational Assignment. Assuming that the shift of a vibrational peak in a MATI spectrum due to the applied electric field is similar to that of the 0−0 band, the vibrational frequency of the cation corresponding to each peak can be estimated simply by taking the difference of its position from that of the 0−0 band. The vibrational frequency scale with the origin at the 0−0 band position is also shown in Figure 2. The vibrational frequencies of the cation in the $\tilde{A}^2A'$ state thus obtained are listed in Table 2.

The vinyl chloride cation has 12 nondegenerate normal modes, $\nu_1-\nu_9$ belonging to a' and $\nu_{10}-\nu_{12}$ to a'' following the Mulliken notation. Main characters of the a' modes are as

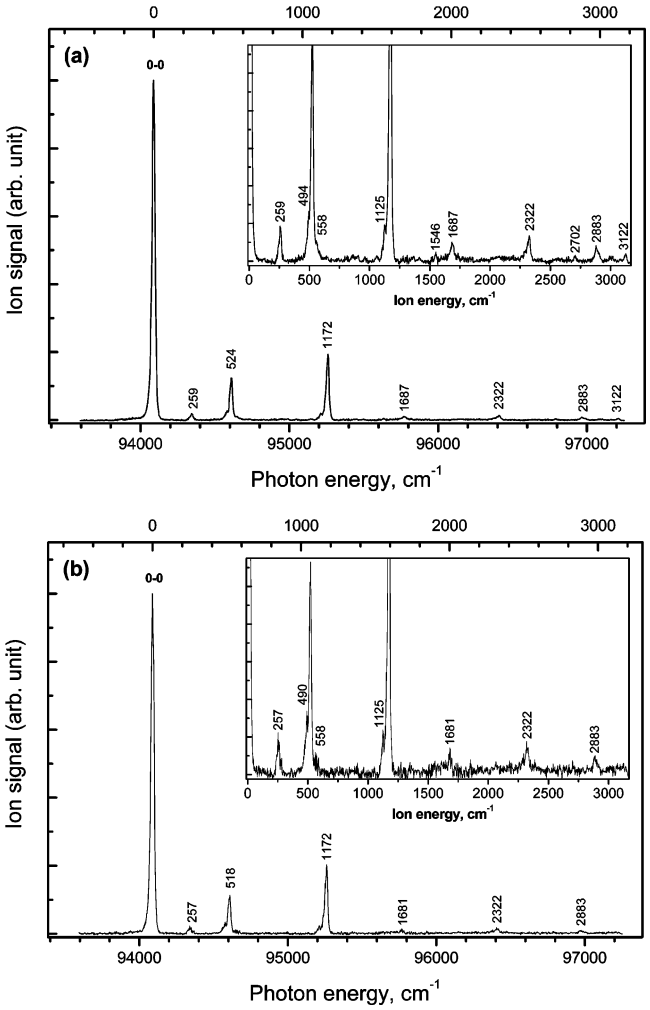

Figure 2. One-photon MATI spectrum of vinyl chloride recorded by monitoring (a) $C_2H_3{}^{35}Cl^+$ and (b) $C_2H_3{}^{37}Cl^+$ in the first excited electronic state ($\tilde{A}^2A'$). The *x*-scale at the top of the figure corresponds to the vibrational frequency scale for the cation. Its origin is at the 0−0 band position. Spectra magnified by 10 along the *y* axis are shown as insets.

TABLE 3: Ionization Energy to the $\tilde{A}^2A'$ State of Vinyl Chloride Cation, in eV

	IE ($\tilde{A}^2A'$)	
$C_2H_3{}^{35}Cl$	11.6667 ± 0.0006	this work
$C_2H_3{}^{37}Cl$	11.6670 ± 0.0006	this work
C_2H_3Cl	11.664 ± 0.005	PES, ref 37
C_2H_3Cl	11.672 ± 0.005	TPES, ref 37
C_2H_3Cl	11.64 ± 0.03	PES, ref 47

follows. ν_1 and ν_2 are asymmetric and symmetric $C_1-H_{1,2}$ stretching vibrations, respectively, ν_3 is C_2-H_3 stretching, ν_4 is C_1-C_2 stretching, ν_5 is $H_1C_1H_2$ bending, ν_6 is $C_1C_2H_3$ bending, ν_7 is $C_2C_1H_{1,2}$ bending, ν_8 is C_2-Cl stretching, and ν_9 is C_1C_2Cl bending. The a'' modes are out-of-plane vibrations involving mostly hydrogen motions.[40]

Overall pattern of the MATI spectrum to the $\tilde{A}^2A'$ state of vinyl chloride cation is similar to that of vinyl bromide.[15] By referring to the quantum chemical results presented above and by comparing with the assignments for the vibrations of $C_2H_3Br^+$ in the first excited electronic state, it was rather straightforward to assign the two prominent peaks at 524 and 1172 cm^{-1} to 8^1 and 6^1, respectively. It is to be noted, however, that the observed frequencies are quite different from the calculated values, 524 vs 572 cm^{-1} for 8^1 and 1172 vs 1227 cm^{-1} for 6^1, representing inaccuracy in the excited-state calculation by TDDFT. In the case of 8^1 for $C_2H_3Br^+$ in the first excited electronic state,[15] $\tilde{A}^2A'$, the corresponding values were 468 and 504 cm^{-1}, respectively. In contrast, the 8^1 frequency in the ground electronic state of $C_2H_3Br^+$, $\tilde{X}^2A''$, calculated by DFT was in better agreement with the experimental value, 700 vs 689 cm^{-1}.[38] Despite the substantial differences between experimental and calculated frequencies, the isotope shifts were well predicted by calculations, which helped positive identification of the above peaks, 8^1 in particular.

Since 6^1 and 8^1 were dominant in the MATI spectrum, the overtones and combinations of ν_6 and ν_8 were assigned before identifying other fundamentals. Accordingly, the peaks at 1687 and 2322 cm^{-1} were assigned to 6^18^1 and 6^2, respectively. Even though 8^2 was expected at or somewhat below 1048 cm^{-1}, its positive identification was not possible. Other fundamentals lying below 1700 cm^{-1} could be identified by referring to the calculated frequencies and to the corresponding values in the MATI spectrum of C_2H_3Br in the $\tilde{A}^2A'$ state. These were 9^1, 12^1, and 4^1 at 259, 558, and 1546 cm^{-1}, respectively. The calculated frequencies for these peaks were 303, 598, and 1628 cm^{-1}, respectively, while those in the $C_2H_3Br^+$ vibrational spectrum were 270, 566, and 1566 cm^{-1}. Then, the peaks at 494, 1125, and 2702 cm^{-1} could be assigned to 9^2, 12^2, and 4^16^1. Other than 4^16^1 at 2702 cm^{-1}, two distinct peaks were observed in the 3000 cm^{-1} region, namely at 2883 and 3122 cm^{-1}. Reasonable assignment of these peaks to overtones or combinations of vibrations appearing below 1700 cm^{-1} was not possible. Referring to the calculated frequencies and Franck−Condon factors, their most reasonable assignments were 3^1 and 1^1, respectively. To summarize, seven out of 12 fundamentals were identified in the MATI spectrum.

D. Determination of the Excited-State Geometry via Franck−Condon Fit. As a part of our effort for spectral assignment, Franck−Condon factors were evaluated using the molecular parameters obtained by quantum chemical calculations. Then the MATI spectrum for generation of $C_2H_3Cl^+$ in the $\tilde{A}^2A'$ state was simulated utilizing the experimental bandwidth. The molecular parameters used were the geometries, the vibrational frequencies, and the normal mode eigenvectors for the neutral and the cation. These were obtained at the DFT/B3LYP and TDDFT/B3LYP levels, respectively. The simulated spectrum obtained using the parameters calculated with the 6-311++G(3df,3pd) basis set is shown in Figure 3(b). The experimental MATI spectrum is shown in Figure 3(a) for comparison. Even though the two spectra look strikingly different, it is obvious that the differences are mostly due to the differences in the intensities of 9^1, 8^1, and related combinations. Namely, 9^1 is much stronger, while 8^1 is much weaker in the simulated spectrum than in the experimental one. One of the possible reasons for the discrepancy in the intensity pattern between experimental and calculated ZEKE/MATI spectra is the participation of channel interaction.[41−43] Namely, peaks in low-frequency region may gain intensity at the cost of those in high-frequency region through intensity borrowing.[41] However, the fact that 8^1 is stronger than 9^1 in the experimental spectra is not compatible with such an explanation. Hence, it is very likely that the observed discrepancy is due to the inaccuracy in molecular parameters obtained by quantum chemical calculations, especially those for the cation in the $\tilde{A}^2A'$ state, rather than the occurrence of channel interaction.

It is extremely difficult to determine the geometry of a cation in an excited electronic state. Also, it is well-known that excited-state geometries obtained by quantum chemical calculations are generally inaccurate.[44] Recently, we reported a method to

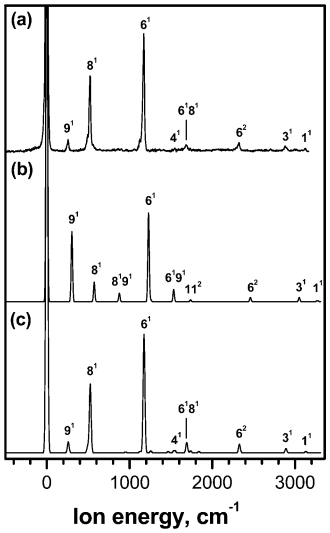

Figure 3. (a) One-photon MATI spectrum of C_2H_3Cl. (b) A spectrum simulated by using the Franck−Condon factors calculated with the molecular parameters obtained at the B3LYP/6-311++G(3df,3pd) level. (c) The simulated spectrum obtained via Franck−Condon fitting (see text for details).

determine the equilibrium geometry of a cation via Franck−Condon fitting of its MATI spectrum.[24,25] Experimentally determined geometry of the corresponding neutral and experimental vibrational frequencies of the neutral and the cation were used in the fitting. Since the normal mode eigenvectors for the neutral and the cation were not generally available, those obtained at various quantum chemical levels were used. It was found that the quantum chemical levels used to calculate the eigenvectors hardly affected the final results.[25] Then, the cation geometry was determined by adjusting the bond lengths and the bond angles until the simulated spectrum agreed with the experimental MATI spectrum. The same has been attempted in this work for $C_2H_3Cl^+$ in the $\tilde{A}^2A'$ state. Cation symmetry in this state was assumed to be C_s, eliminating dihedral angles from the list of adjustable parameters. The bond lengths $r(C_1H_1)$ and $r(C_1H_2)$ could not be determined because only the intensity of 1^1 was available for their determination. Instead, we calculated the Franck−Condon factors for this fundamental using the $r(C_1H_1)$ and $r(C_1H_2)$ bond lengths obtained at the TDDFT level. The result was in agreement with the experimental intensity within its error limit. Hence, these bond lengths were no longer treated as adjustable parameters. Under the assumption of C_s symmetry, two out of three bond angles involving C_1 were adjustable. However, 5^1 and 7^1 which might have been affected by the geometry change along these bond angles did not appear in the MATI spectrum. Using the DFT values for the neutral and the TDDFT values for the cation, the Franck−Condon factors of 5^1 and 7^1 became extremely small, suggesting the changes in these bond angles were well predicted by the calculations. Using the experimental bond angles for the neutral[43] instead of the DFT values, however, resulted in the 5^1 and 7^1 Franck−Condon factors with noticeable magnitudes. Hence, these bond angles in the cation were adjusted such that their changes from the experimental data for the neutral were the same as the respective calculated changes. Eliminating the above geometrical parameters left $r(C_1C_2)$, $r(C_2H_3)$, $r(C_2Cl)$, $\angle C_1C_2H_3$, and $\angle C_1C_2Cl$ as adjustable parameters.

The best Franck−Condon fit thus achieved for the MATI spectrum in Figure 3(a) is shown in Figure 3(c). It is to be noted that the experimental spectrum could be reproduced by simulation even to minor details. The geometrical parameters for $C_2H_3Cl^+$ in the $\tilde{A}^2A'$ state thus determined are listed in Table 1. It is to be mentioned that the accuracy of the molecular parameters determined here depends on the accuracy of the intensities of the MATI peaks relative to that of the 0−0 band. In the present case, the intensities of the fundamentals, overtones, and combinations could be determined rather reliably. The intensity of the 0−0 band was rather inaccurate, however, due to a dip in the VUV laser output at this position. Repeated experiments showed that it might be inaccurate by as much as ±30%. The error limits to the geometrical parameters estimated with this fluctuation are shown in Table 1. It is to be noted that the errors were not significant even when the intensity of the 0−0 band and, hence, the normalized intensities of other peaks also were rather inaccurate. The eigenvectors obtained at the TDDFT/B3LYP level with other basis sets were also used in Franck−Condon fitting. The results were essentially the same as the above and are not presented here.

All the geometrical data determined by Franck−Condon fitting except $r(C_2H_3)$ show significant differences from the corresponding data in the TDDFT results. In the cases of $r(C_1C_2)$ and $\angle C_1C_2H_3$, differences between the calculated (TDDFT) and experimental (Franck−Condon fitting) results in the cation are rather similar to the corresponding differences in the neutral. This explains why the intensities of the associated fundamentals, 4^1 and 6^1, in the MATI spectrum are fairly well reproduced in the spectrum simulated with the quantum chemical data, Figure 3(b). In contrast, the calculated $\angle C_1C_2Cl$ bond angles in the neutral and the cation are widely different from the experimental data, the calculated angle being larger than the experimental one for the neutral while the opposite being the case in the cation. This has resulted in erroneously strong intensity for 9^1 in the simulated spectrum in Figure 3(b).

V. Summary and Conclusion

It is expected to be difficult to record the vibrational spectra of aliphatic halide cations in the ground electronic state by conventional two-photon ZEKE/MATI because the first excited electronic states of the corresponding neutrals are usually dissociative.[46] Recording the vibrational spectra in upper electronic states by the same technique would be virtually impossible. Using the powerful VUV output in the 107−102.8 nm region generated by the home-built Hg four-wave mixing light source, the vibrational spectrum of $C_2H_3Cl^+$ in the $\tilde{A}^2A'$ state was successfully recorded via one-photon MATI in this work. The resolution was much better than that in a recent PES study, and even very weak peaks could be identified. It is ironic that the vibrational spectrum of $C_2H_3Cl^+$ in the ground electronic state, $\tilde{X}^2A''$, has not been reported yet. In fact, we attempted to record the ground-state spectrum but failed because the light source used had very weak output over a 500 cm^{-1} wide spectral region covering the 0−0 band.

The geometry of the cation in the $\tilde{A}^2A'$ state was determined by Franck−Condon fitting of the MATI spectrum. The cation geometry thus determined was noticeably different from those optimized at the TDDFT level. Hence, not only the ionization energy and the vibrational frequencies but also the geometrical data determined in this work may be regarded as useful benchmark data in the development of quantum chemical methods for excited-state calculation.

As has been mentioned already, our previous charge exchange study suggested that the $\tilde{A}^2A'$ state of $C_2H_3Cl^+$ did not undergo radiative or radiationless relaxation easily and survive even several microseconds after its formation. However, the spectral resolution achieved in this work is not sufficient to determine

the lifetime of the state. Also, even though the pulsed-field ionization was performed a few ten microseconds after excitation, this does not mean that the neutral with the ion core state of $\tilde{A}^2A'$ survived during this period because the Rydberg (or ZEKE) neutral can survive even when changes occur in the ion core. An experimental method is being sought to confirm the very long lifetime of this cation state.

Acknowledgment. This work was financially supported by CRI, Ministry of Science and Technology, Republic of Korea. M.L. thanks the Ministry of Education for the Brain Korea 21 fellowship.

References and Notes

(1) Laane, J.; Takahashi, H.; Bandrauk, A. *Structure and Dynamics of Electronic Excited State*; Springer-Verlag: Berlin, 1999.

(2) McGowan, J. W. *The Excited State in Chemical Physics*; Wiley: New York, 1981.

(3) Bartolo, B. D. *Spectroscopy of the Excited State*; Plenum Press: New York, 1976.

(4) Klessinger, M.; Michl, J. *Excited States and Photochemistry of Organic Molecules*; VCH Publisher: New York, 1995.

(5) Kimura, K.; Katasumata, S.; Achiba, Y.; Yamazaki, T.; Iwata, S. *Handbook of HeI Photoelectron Spectra of Fundamental Organic Molecules*; Japan Scientific Societies Press: Tokyo, 1981.

(6) Turner, D. W.; Baker, C.; Baker, A. D.; Brundle, C. R. *Molecular Photoelectron Spectroscopy*; Wiley: New York, 1970.

(7) Yang, J.; Mo, Y.; Lau, K. C.; Song, Y.; Qian, X. M.; Ng, C. Y. *Phys. Chem. Chem. Phys.* **2005**, *7*, 1518.

(8) Seiler, R.; Hollenstein, U.; Softley, T. P.; Merkt, F. *J. Chem. Phys.* **2003**, *118*, 10024.

(9) Sohnlein, B. R.; Li, S.; Fuller, J. F.; Yang, D. S. *J. Chem. Phys.* **2005**, *123*, 014318.

(10) Park, S. T.; Kim, S. K.; Kim, M. S. *Nature (London)* **2002**, *415*, 306.

(11) Burrill, A. B.; Chung, Y. K.; Mann, H. A.; Johnson, P. M. *J. Chem. Phys.* **2004**, *120*, 8587.

(12) Georgiev, S.; Neusser, H. J. *J. Electron Spectrosc. Relat. Phenom.* **2005**, *142*, 207.

(13) Lee, M.; Kim, H.; Lee, Y. S.; Kim, M. S. *Angew. Chem., Int. Ed.* **2005**, *44*, 2929.

(14) Kwon, C. H.; Kim, H. L.; Kim, M. S. *J. Chem. Phys.* **2002**, *116*, 10361.

(15) Lee, M.; Kim, M. S. *J. Chem. Phys.* **2005**, *123*, 174310.

(16) Müller-Dethlef, K. *J. Electron Spectrosc. Relat. Phenom.* **1995**, *75*, 35.

(17) Li, C.; Lin, J. L.; Tzeng, W. B. *J. Chem. Phys.* **2005**, *122*, 044311.

(18) He, Y.; Wu, C.; Kong, W. *J. Chem. Phys.* **2004**, *121*, 8321.

(19) Taylor, D. P.; Goode, J. G.; LeClaire, J. E.; Johnson, P. M. *J. Chem. Phys.* **1995**, *103*, 6293.

(20) Goode, J. G.; Hofstein, J. D.; Johnson, P. M. *J. Chem. Phys.* **1997**, *107*, 1703.

(21) Kong, W.; Rodgers, D.; Hepburn, J. W. *J. Chem. Phys.* **1993**, *99*, 8571.

(22) Hepburn, J. W. *J. Chem. Phys.* **1997**, *107*, 7106.

(23) Merkt, F.; Mackenzie, S. R.; Rednall, R. J.; Softley, T. P. *J. Chem. Phys.* **1993**, *99*, 8430.

(24) Lee, M.; Kim, H.; Lee, Y. S.; Kim, M. S. *J. Chem. Phys.* **2005**, *122*, 244319.

(25) Bae, Y. J.; Lee, M.; Kim, M. S. *J. Phys. Chem. A* **2006**, in press.

(26) Saunders: K. J. *Organic Polymer Chemistry*; Chapman and Hill, New York, 1988.

(27) Minsker, K. S.; Kolesov, S. V.; Zaikov, G. E. *Degradation and Stabilization of Vinyl Chloride Based Polymers*; Pergamon Press: Oxford, 1988.

(28) Isidrov, V. A. *Organic Chemistry of the Earth's Atmosphere*; Springer-Verlag: Berlin, 1990.

(29) Marini-bettòlo, G. B. *Chemical Events in the Atmosphere and Their Impact on the Environment*; Elsevier: New York, 1986.

(30) Yoon, S. H.; Choe, J. C.; Kim, M. S. *Int. J. Mass Spectrom.* **2003**, *227*, 21.

(31) Youn, Y. Y.; Choe, J. C.; Kim, M. S. *J. Am. Soc. Mass Spectrom.* **2003**, *14*, 110.

(32) Myers, A. B.; Rizzo, T. R. *Laser Techniques in Chemistry*; John Wiley & Son: New York, 1995; Chapter 5, pp 149−183.

(33) Hepburn, J. W. *Chem. Soc. Rev.* **1996**, *25*, 281.

(34) Rupper, P.; Zehnder, O.; Merkt, F. *J. Chem. Phys.* **2004**, *121*, 8279.

(35) Frisch, M. J.; Trucks, G. W.; Schlegel, H. B.; Scuseria, G. E.; Robb, M. A.; Cheeseman, J. R.; Zakrzewski, V. G.; Montgomery, J. A., Jr.; Stratmann, R. E.; Burant, J. C.; Dapprich, S.; Millam, J. M.; Daniels, A. D.; Kudin, K. N.; Strain, M. C.; Farkas, O.; Tomasi, J.; Barone, V.; Cossi, M.; Cammi, R.; Mennucci, B.; Pomelli, C.; Adamo, C.; Clifford, S.; Ochterski, J.; Petersson, G. A.; Ayala, P. Y.; Cui, Q.; Morokuma, K.; Malick, D. K.; Rabuck, A. D.; Raghavachari, K.; Foresman, J. B.; Cioslowski, J.; Ortiz, J. V.; Stefanov, B. B.; Liu, G.; Liashenko, A.; Piskorz, P.; Komaromi, I.; Gomperts, R.; Martin, R. L.; Fox, D. J.; Keith, T.; Al-Laham, M. A.; Peng, C. Y.; Nanayakkara, A.; Gonzalez, C.; Challacombe, M.; Gill, P. M. W.; Johnson, B.; Chen, W.; Wong, M. W.; Andres, J. L.; Gonzalez, C.; Head-Gordon, M.; Replogle, E. S.; Pople, J. A. *Gaussian 98, revision A.6*; Gaussian Inc.: Pittsburgh, PA, 1998.

(36) Sharp, T. E.; Rosenstock, H. M. *J. Chem. Phys.* **1963**, *41*, 3453.

(37) Locht, R.; Leyh, B.; Hottmann, K.; Baumgärtel, H. *Chem. Phys.* **1997**, *220*, 217.

(38) Lee, M.; Kim, M. S. *J. Chem. Phys.* **2003**, *119*, 5085.

(39) Kwon, C. H.; Kim, H. L.; Kim, M. S. *J. Chem. Phys.* **2003**, *119*, 215.

(40) Sverdlov, L. M.; Kovner, M.; Karinov, E. *Vibrational Spectra of Polyatomic Molecules*; Wiley: New York, 1974.

(41) Schlag, E. W. *ZEKE Spectroscopy*; Cambridge University Press: Cambridge, 1998.

(42) Chupka, W. A.; Grant, E. R. *J. Phys. Chem. A* **1999**, *103*, 6127.

(43) Yeretzian, C.; Hermann, R. H.; Ungar, H.; Selzle, H. L.; Schlag, E. W.; Lin, S. H. *Chem. Phys. Lett.* **1995**, *239*, 61.

(44) Serrano-Andrés, L.; Merchán, M. *J. Mol. Struct.* **2005**, *729*, 99.

(45) Hayashi, M.; Inagusa, T. *J. Mol. Struct.* **1990**, *220*, 103.

(46) Herzberg, G. *Molecular Spectra and Molecular Structure*; Van Nostrand Reinhold: New York, 1945; Vol. III.

(47) Sze, K. H.; Brion, C. E.; Katrib, A.; El-issa, B. *Chem. Phys.* **1989**, *137*, 369.